ULAM SETS WHOSE INITIAL VECTORS DEPEND ON φ

MAXIE D. SCHMIDT
SCHOOL OF MATHEMATICS
GEORGIA INSTITUTE OF TECHNOLOGY
ATLANTA, GA 30332 USA
MAXIEDS@GMAIL.COM

1. Kravitz and Steinerberger's article

The authors define generalized Ulam sets in higher dimensions for a set of initial starting vectors, $\{v_1, \ldots, v_k\} \subseteq \mathbb{R}^n_{\geq 0}$. Ulam was interested in determining properties of his quasi-periodic sequence such as its asymptotic density which can only be estimated empirically. We can ask related natural questions about the generalized sequences. The article provides many example plots in 2D with differing initial vectors to demonstrate cases where we have completely predictable behavior to cases which exhibit both chaotic and regular behavior (like out special case below). Notable, the authors provide a lattice theorem in Section 2 of the article which classifies some behavior of the 2D sequences with two initial vectors (our cases). Special case sequence proofs of form are also outlined in Section 2. The authors provide one further example of a generalization to 3D vectors in this section. The last sections of the paper focus on a hodge-podge of topics including the independence of norms used to determine minimal vectors and attempting to classify 2D behavior such as column doubling and periodicity. The plethora of examples cited in the article make is easy for the reader to get a good grounding on the generalized, especially 2D, Ulam set forms.

2. Steinerberger's hidden signals article

Stienerberger again considers the ordinary 1D Ulam sequence, $\{1, 2, 3, 4, 6, 8, 11, 13, 16, 18, 26, \ldots\}$, but this time in the context of so-termed "*hidden signals*" in the Fourier-like plots involving the sequence. In particular, for an empirically discovered $\alpha \sim 2.5714474995$ Steinerberger found that the set

$$\{\alpha a_n \bmod 2\pi : n \in \mathbb{N}\}$$

generates an absolutely continuousnon-uniform measure supported on a subset of $\mathbb{T}$ (what is $\mathbb{T}$?). Correspondingly, all but very select few of the first 10^7 elements of the Ulam set satisfy $\cos(\alpha a_n) < 0$. If we define, as in the article, the function

$$f_N(x) := \sum_{n=1}^{N} \cos(a_n x),$$

we have not that $|f_N(x)| \sim \sqrt{N}$ as expected away from $x = 0$, but in fact that $f_N(\alpha) \sim -0.8N$, which is an indicator of a hidden signal. This hidden signal is reflected in the (histogram) distribution plot of the set

$$S_N = \left\{ \alpha a_n - 2\pi \left\lfloor \frac{\alpha a_n}{2\pi} \right\rfloor \right\},$$

which has a two peak phenomenon with one peak occurring at α. The author also considers other Ulam sets with differing initial conditions and a few notable examples in a related context.

3. Some work on sequence 2

3.1. **Definition of the sequence and example elements.** For the first sequence with initial values, $(1, \varphi), (\varphi, 1)$ we have the following examples of set elements for $N := 35$:

```
ULAM SET:  [(1, golden_ratio), (golden_ratio, 1), (golden_ratio + 1, golden_ratio + 1),
(golden_ratio + 2, 2*golden_ratio + 1), (2*golden_ratio + 1, golden_ratio + 2),
(golden_ratio + 3, 3*golden_ratio + 1), (golden_ratio + 4, 4*golden_ratio + 1),
(3*golden_ratio + 1, golden_ratio + 3), (golden_ratio + 5, 5*golden_ratio + 1),
(4*golden_ratio + 1, golden_ratio + 4), (golden_ratio + 6, 6*golden_ratio + 1),
```

Date: Sunday 18th June, 2017.

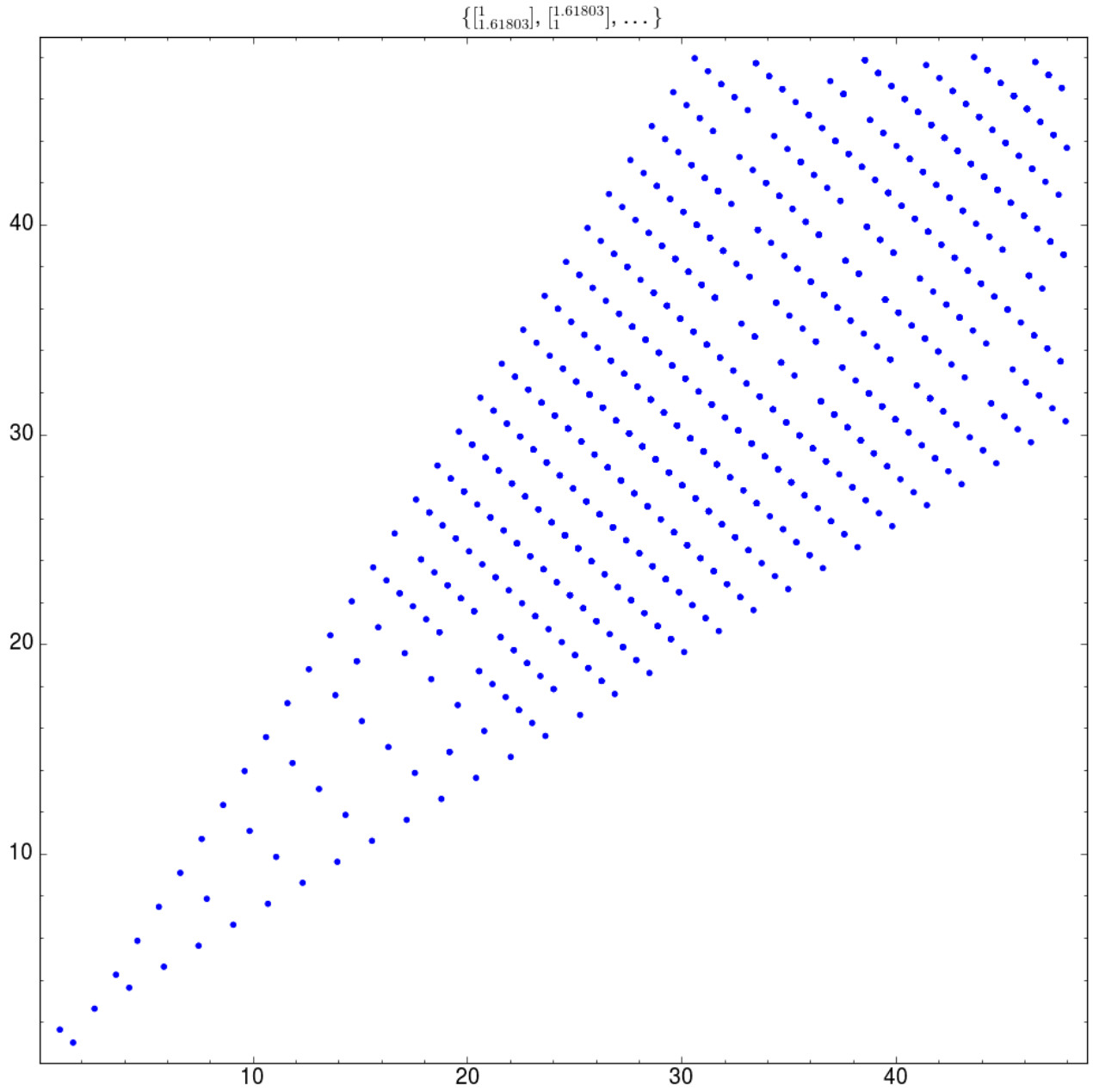

Figure 3.1. *The second Ulam set variant when* $N := 500$.

```
(3*golden_ratio + 3, 3*golden_ratio + 3), (golden_ratio + 7, 7*golden_ratio + 1),
(5*golden_ratio + 1, golden_ratio + 5), (golden_ratio + 8, 8*golden_ratio + 1),
(3*golden_ratio + 5, 5*golden_ratio + 3), (golden_ratio + 9, 9*golden_ratio + 1),
(6*golden_ratio + 1, golden_ratio + 6), (5*golden_ratio + 3, 3*golden_ratio + 5),
(golden_ratio + 10, 10*golden_ratio + 1), (3*golden_ratio + 7, 7*golden_ratio + 3),
(7*golden_ratio + 1, golden_ratio + 7), (golden_ratio + 11, 11*golden_ratio + 1),
(5*golden_ratio + 5, 5*golden_ratio + 5), (golden_ratio + 12, 12*golden_ratio + 1),
(3*golden_ratio + 9, 9*golden_ratio + 3), (8*golden_ratio + 1, golden_ratio + 8),
(7*golden_ratio + 3, 3*golden_ratio + 7), (golden_ratio + 13, 13*golden_ratio + 1),
(5*golden_ratio + 7, 7*golden_ratio + 5), (9*golden_ratio + 1, golden_ratio + 9),
(golden_ratio + 14, 14*golden_ratio + 1), (3*golden_ratio + 11, 11*golden_ratio + 3),
(7*golden_ratio + 5, 5*golden_ratio + 7), (golden_ratio + 15, 15*golden_ratio + 1),
```

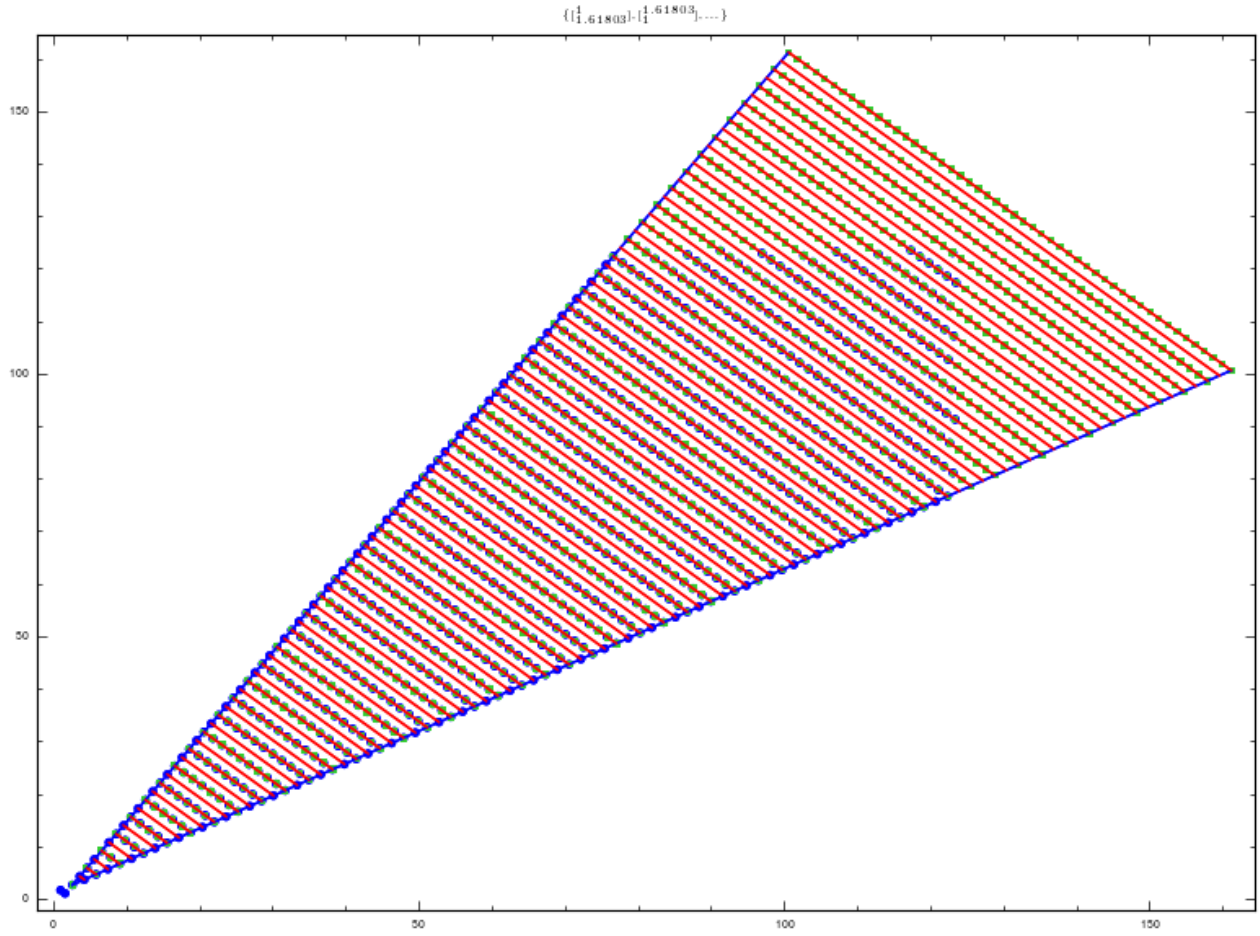

Figure 3.2. *The second Ulam set variant when* $N := 500$ *with bounding lines and lattice points drawn.*

```
(5*golden_ratio + 9, 9*golden_ratio + 5), (10*golden_ratio + 1, golden_ratio + 10),
(9*golden_ratio + 3, 3*golden_ratio + 9), (golden_ratio + 16, 16*golden_ratio + 1),
(3*golden_ratio + 13, 13*golden_ratio + 3), (7*golden_ratio + 7, 7*golden_ratio + 7),
(golden_ratio + 17, 17*golden_ratio + 1), (11*golden_ratio + 1, golden_ratio + 11),
(5*golden_ratio + 11, 11*golden_ratio + 5), (9*golden_ratio + 5, 5*golden_ratio + 9),
(3*golden_ratio + 15, 15*golden_ratio + 3), (7*golden_ratio + 9, 9*golden_ratio + 7),
(12*golden_ratio + 1, golden_ratio + 12), (11*golden_ratio + 3, 3*golden_ratio + 11),
(5*golden_ratio + 13, 13*golden_ratio + 5), (9*golden_ratio + 7, 7*golden_ratio + 9),
(13*golden_ratio + 1, golden_ratio + 13), (7*golden_ratio + 11, 11*golden_ratio + 7),
(11*golden_ratio + 5, 5*golden_ratio + 11), (9*golden_ratio + 9, 9*golden_ratio + 9),
(14*golden_ratio + 1, golden_ratio + 14), (13*golden_ratio + 3, 3*golden_ratio + 13),
(7*golden_ratio + 13, 13*golden_ratio + 7), (11*golden_ratio + 7, 7*golden_ratio + 11),
(15*golden_ratio + 1, golden_ratio + 15), (9*golden_ratio + 11, 11*golden_ratio + 9),
(13*golden_ratio + 5, 5*golden_ratio + 13), (11*golden_ratio + 9, 9*golden_ratio + 11),
(16*golden_ratio + 1, golden_ratio + 16), (15*golden_ratio + 3, 3*golden_ratio + 15),
(13*golden_ratio + 7, 7*golden_ratio + 13), (17*golden_ratio + 1, golden_ratio + 17)]
```

A plot of the first points in our Ulam set for $N := 500$ is given in Figure 3.1.

3.2. **Conjectures and notes on form.** All elements of this Ulam set are of the form $(a\varphi + b, b\varphi + a)$ for some $a, b \in \mathbb{N}$. Moreover, these a, b depend on sums and/or products of the Fibonacci and Lucas sequences. The first assertion is also easy enough to prove by induction, but is a nice property. The second is a more interesting property defining the structure of these sets to be investigated further.

As the image in Figure 3.2 suggests, we conjecture that all of the vectors in this set lie between two straight lines in the plane, and on the lattice points between two points on these lines at a certain fixed negative slope. We should be able to compute each of these lines and the fixed slope from our experimental data listing above. More precisely, we can formulate that the points in the set on the bounding lines are given by

$$\{(k\varphi+1, \varphi+k) : 0 \leq k \leq n\} \bigcup \{(\varphi+k, k\varphi+1) : 0 \leq k \leq n\},$$

and that all of the interior points in the Ulam set, U_n, are on a line segment connecting $(k\varphi+1, \varphi+k)$ and $(\varphi+k, k\varphi+1)$ for some (the same) integer k. There are $k+1$ points of the lattice

$$\{(a\phi+b, b\phi+a) : a, b \geq 0,\ a, b \text{ odd }\},$$

on this line segment, not all of them in U_n. To distinguish the cases of which of these lattice points are in the Ulam set, we must make further empirical conjectures which we can prove later. The first few lattice points omitted from the lattice points of the form $(a\phi+b, b\phi+a)$ for a, b odd and between the bounding lines are computed as follows:

4. Hidden signals, Fourier transforms, and Laplace transforms

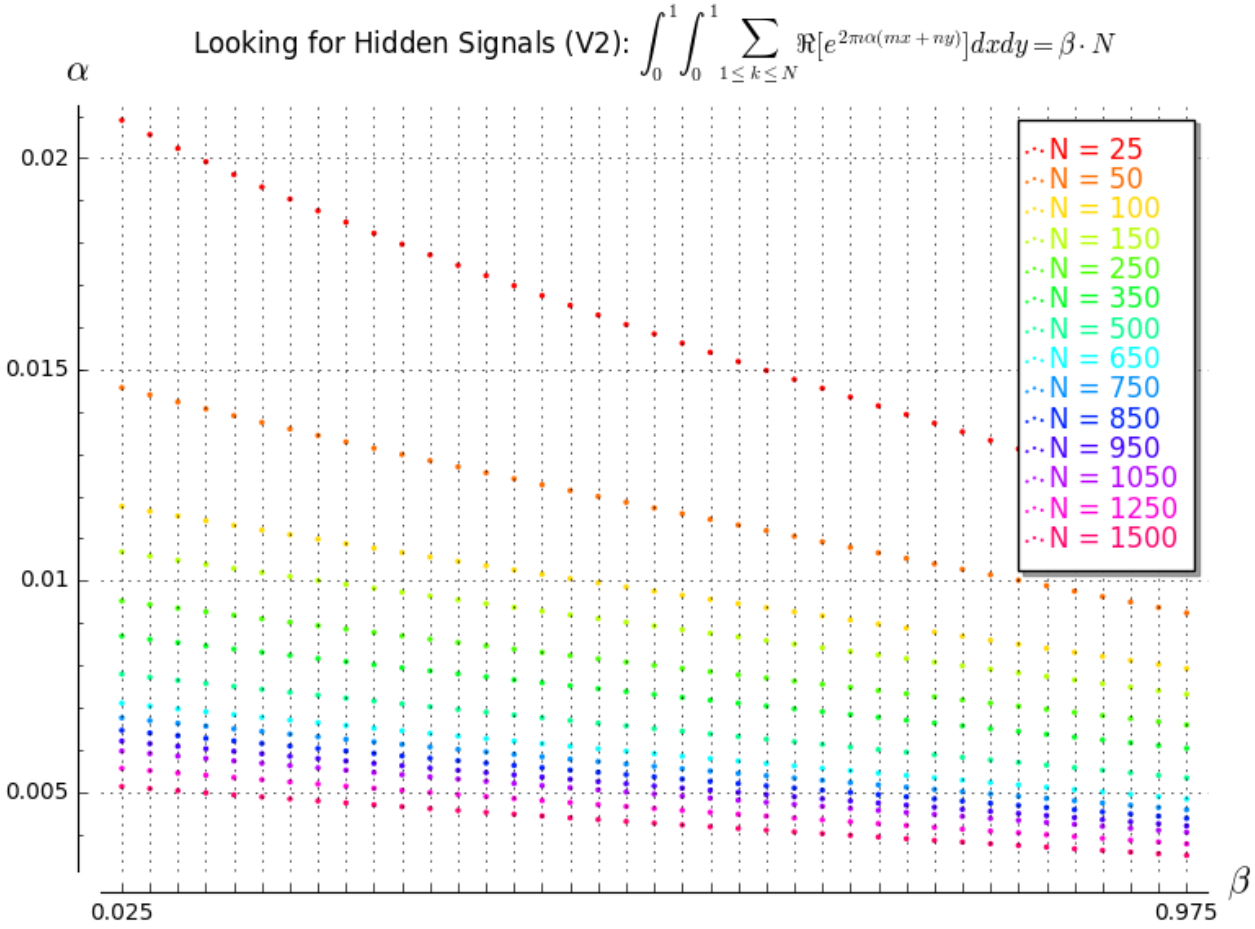

Figure 4.1. *A brute-force approach to identifying hidden signals.*

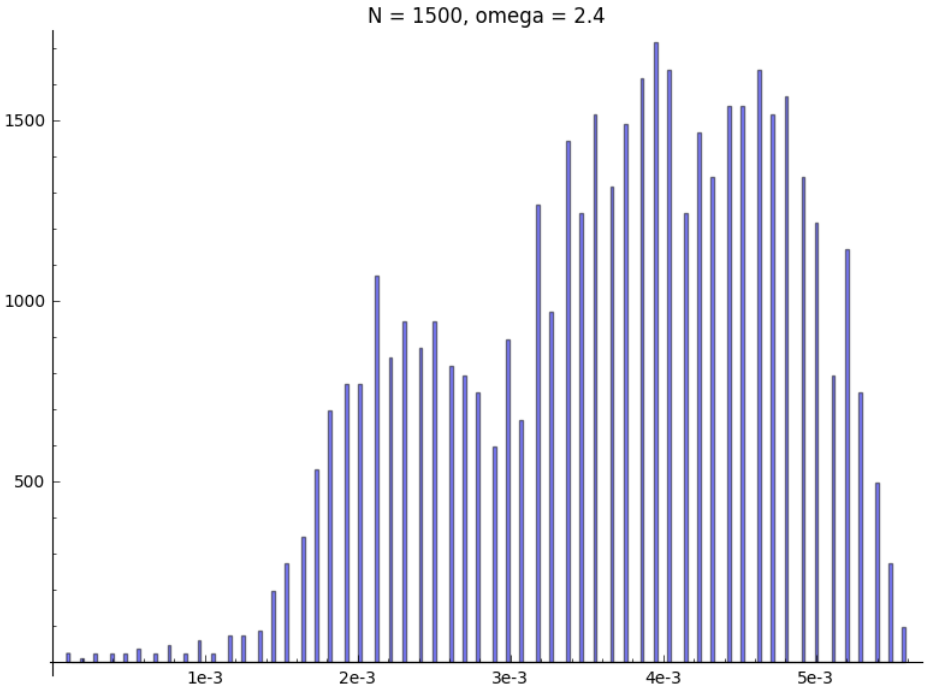

Figure 4.2. $S_{1500}(2.4)$

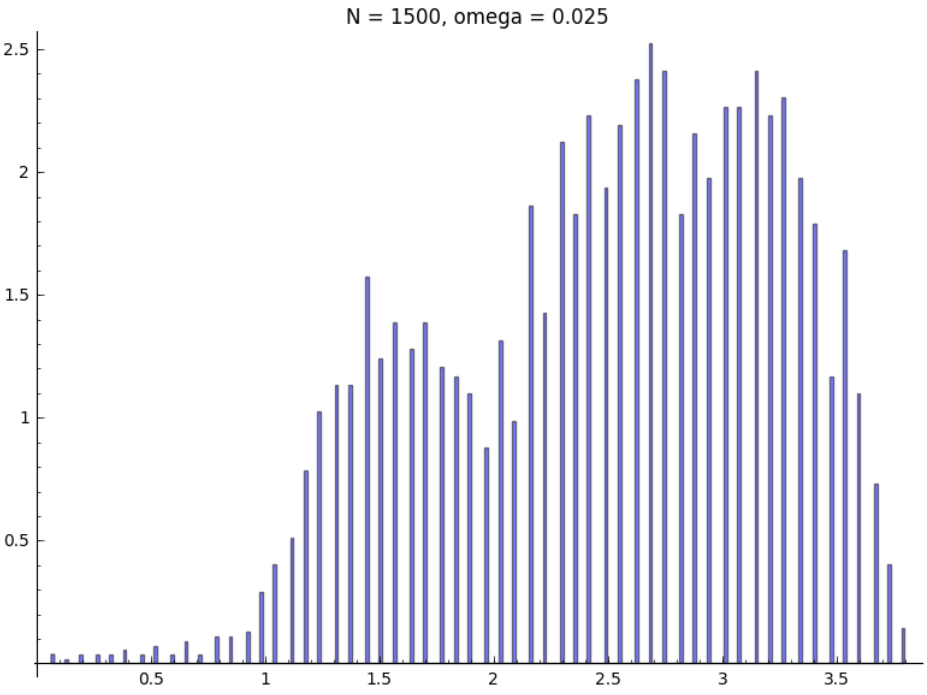

Figure 4.3. $S_{1500}(0.025)$

4.1. **Hidden signal computations.** We have one first computation which attempts (somewhat unsuccessfully) to brute-force the form of the hidden signals shown in Figure 4.1. More in the spirit of the original articles by Steinerberger, we can define the following two sets for some fixed N and a parameter α to visualize the (histogram)

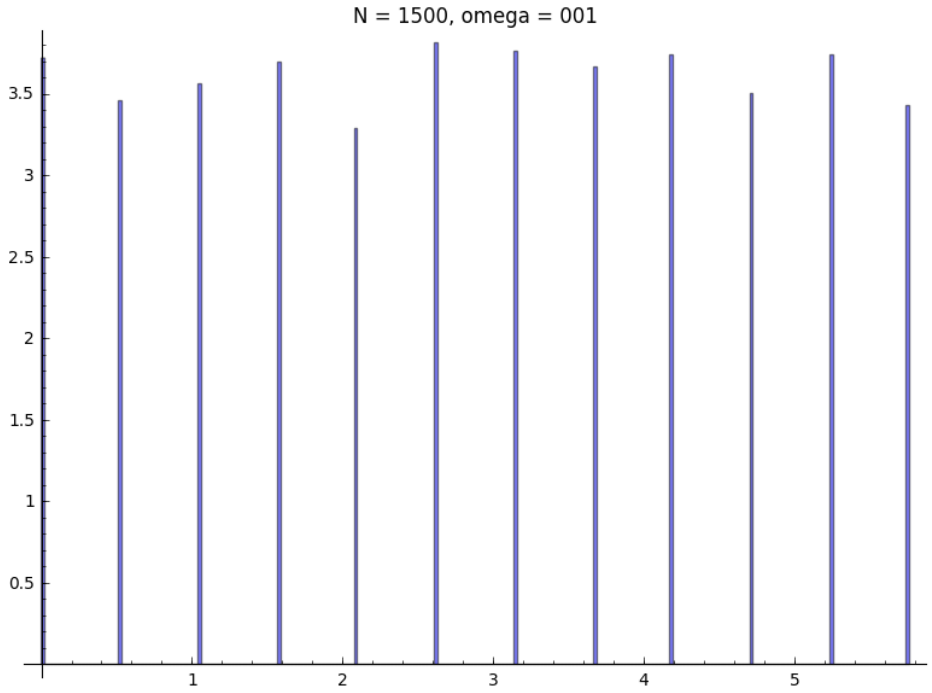

Figure 4.4. $S_{1500}(1.0)$

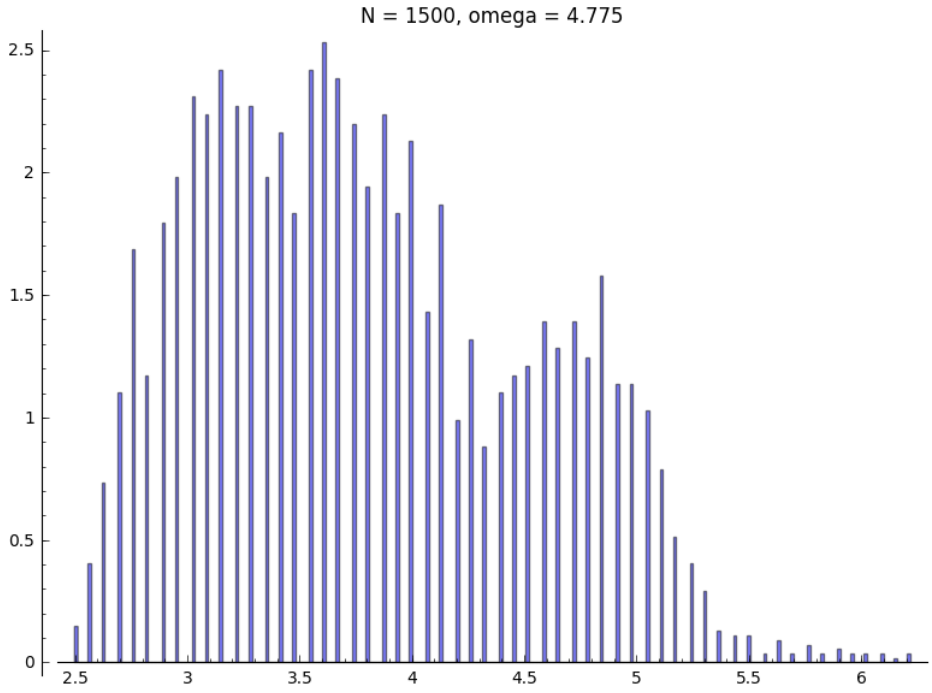

Figure 4.5. $S_{1500}(4.775)$

distribution of these sets for various α:

$$f_N(\alpha) := \sum_{(m,n)\in U_N} \cos(\alpha(m+n))$$

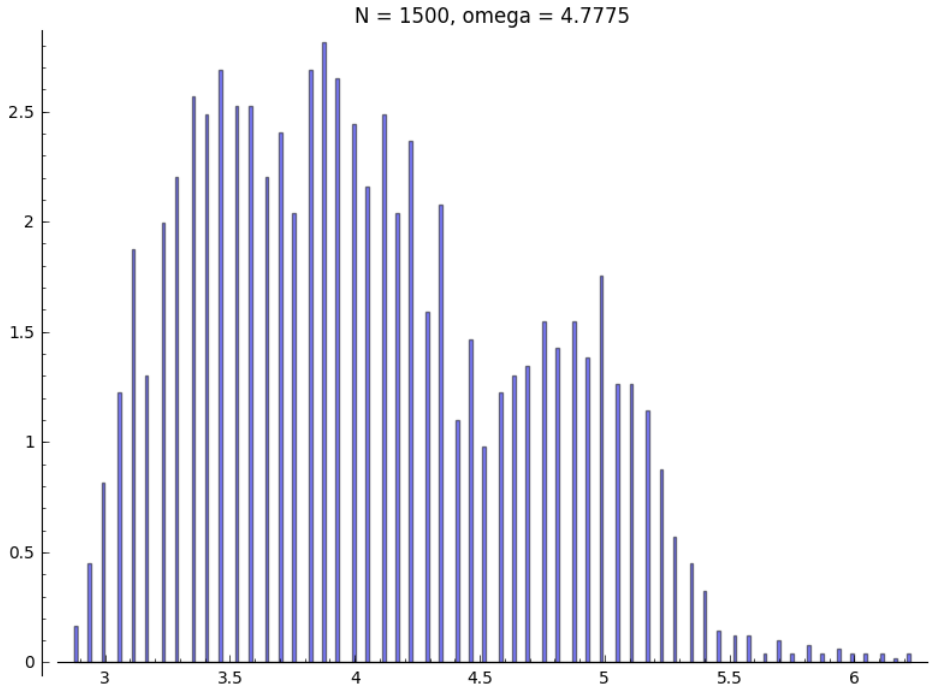

Figure 4.6. $S_{1500}(4.7775)$

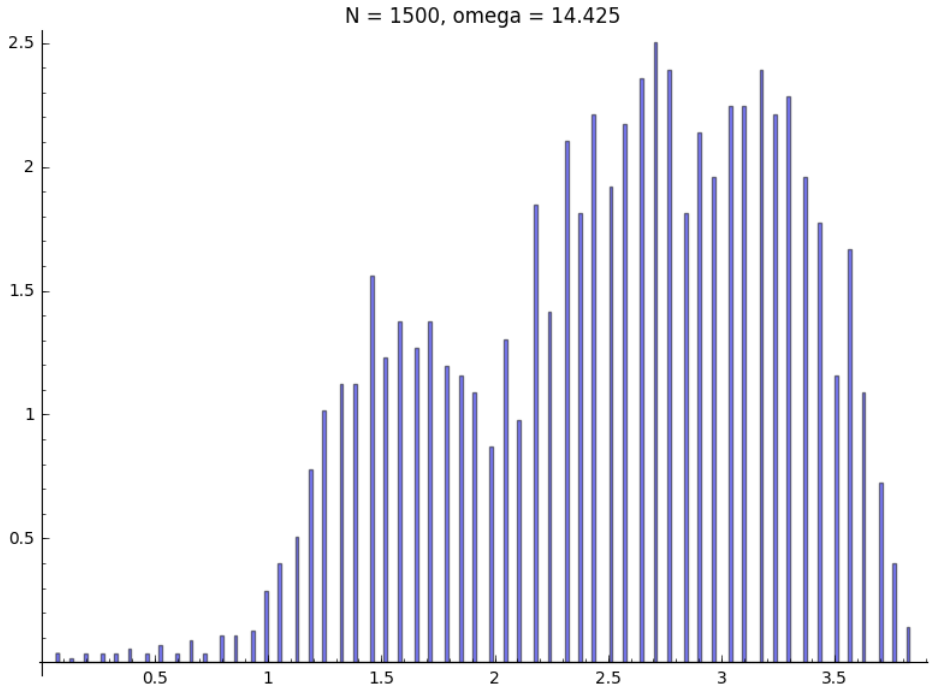

Figure 4.7. $S_{1500}(14.425)$

$$S_N(\alpha) := \left\{ \alpha(m+n) - 2\pi \left\lfloor \frac{\alpha(m+n)}{2\pi} \right\rfloor : (m,n) \in U_N \right\}.$$

The next several figures provide the histogram distributions for various α. In particular, we have discovered numerically that for all $\alpha := 2.4k$ with $k \in \mathbb{Z}^+$ we have that $\cos(\alpha(m+n)) \geq 0$ for all $(m,n) \in U_{2500}$ and these α values

all produce identical histograms to those shown in the figure where

$$\sum_{s\in S_N(2.4k)} s \approx k\cdot C_1\cdot N$$
$$f_N(2.4k)\approx C_2\cdot N,$$

for some constants C_1, C_2. Besides $\alpha = 1$, which was chosen to show a chaotic distribution, the other choices of α were selected by numerical computation which showed that for *most* $(m,n)\in U_N$ $\cos(\alpha(m+n))<0$. The $f_N(\alpha)$ in these cases similarly appears to be proportional to a negative real constant times N. There were no α found such that all (or even with exception of four or less) of the cosine values were negative like in the positive cases which are very clear to identify.

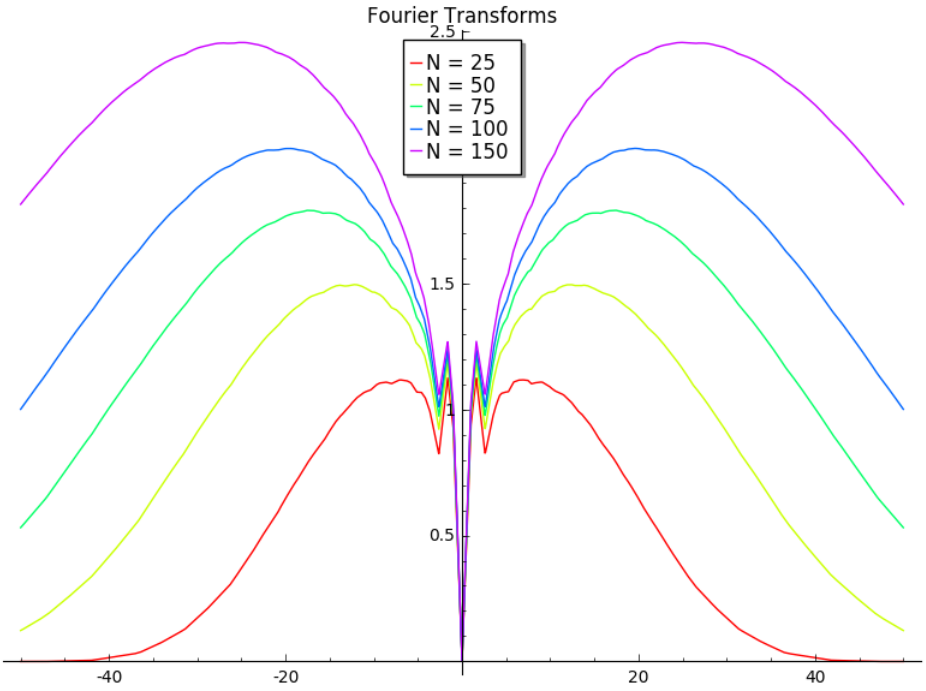

Figure 4.8. *Fourier transform of* $\cos(\alpha(m+n))$ *for* $(m,n)\in U_N$ *for various* N.

4.2. **Fourier transforms and Laplace transforms.** Since

$$\int_0^1\int_0^1 \cos(2\pi\alpha(mx+ny))dxdy = \frac{\sin(\pi\alpha m)\sin(\pi\alpha n)\cos(\pi\alpha(m+n))}{\pi^2\alpha^2 mn},$$

for each $N\geq 1$ we form our Fourier transform (depending on N) to be

$$F_N(\omega) = \sum_{(m,n)\in U_N}\int_{-\infty}^{\infty}\left[\frac{\sin(\pi\alpha m)\sin(\pi\alpha n)\cos(\pi\alpha(m+n))}{\pi^2\alpha^2 mn}\times\exp(2\pi\imath\alpha\omega)\right]d\alpha$$
$$= \sum_{(m,n)\in U_N} -\frac{1}{4mn}\left[-2|\omega|+|m-\omega|+|m+\omega|+|n-\omega|+|n+\omega|-|m+n-\omega|-|m+n+\omega|\right].$$

We can easily see (as in the figures below) that our Fourier transform is symmetric about the line $x=0$. The "*sawtooth*" edges in Figure 4.8 correspond to the points $\omega = 0, \pm\varphi, \pm(\varphi+1)$ by computation. In general, it looks like we will need to scale $F_n(\omega)$ by a function of N piecewise to obtain a limiting distribution as $N\to\infty$. In order to begin to process how to do this analytically, we can form the analogous Fourier transform over all of the Lattice points (our Ulam set is a subset) of the next form for $n\leq N$ when the upper bound N is fixed (when $N\to\infty$ these sums do not converge)

- $(n\varphi+1,\varphi+n)$, $(\varphi+n,n\varphi+1)$ for $1\leq n\leq N$;

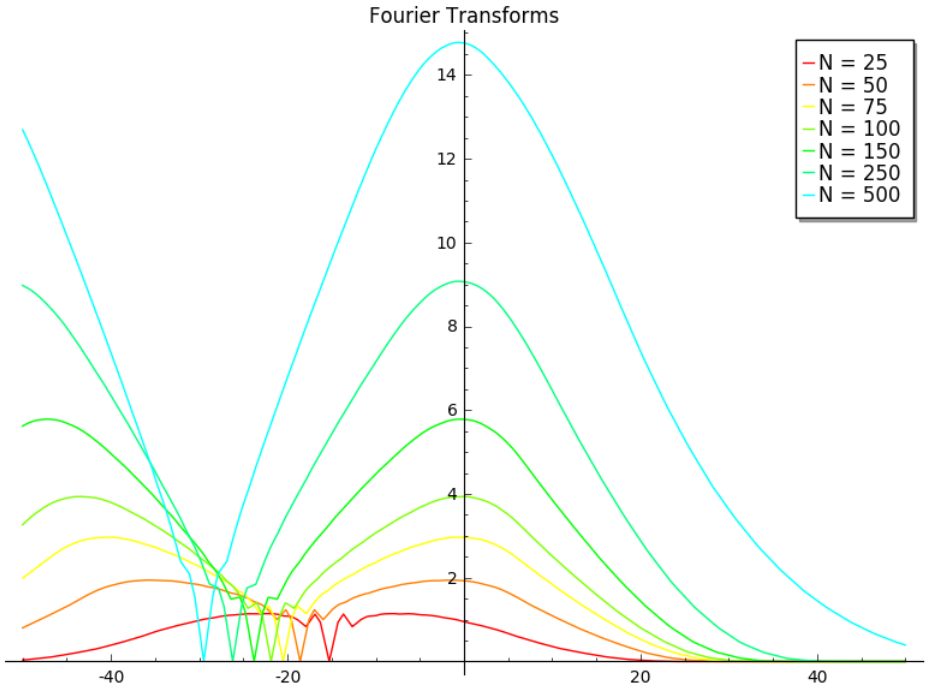

Figure 4.9. *Fourier transform shifted to the left by* $4.745154852900353 * \log(N)$.

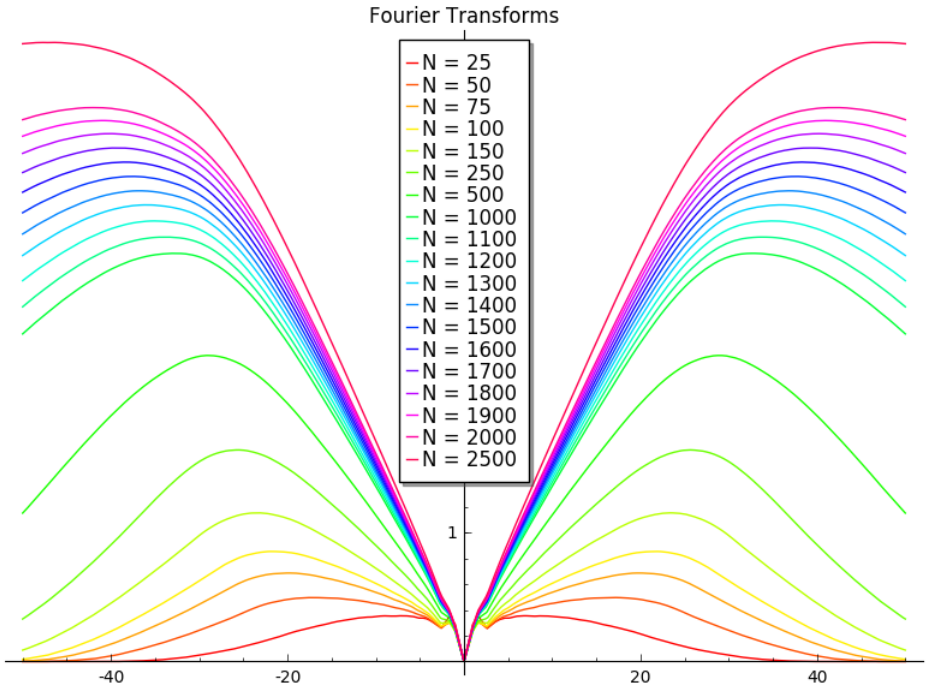

Figure 4.10. *Fourier transform scaled by* $\log(N)$

- $((n+1-b)\varphi+b, b\varphi+n+1-b)$ for $b=2,4,\ldots,n$ when is even and for $b=1,3,\ldots,n$ when n is odd where $1 \leq n \leq N$.

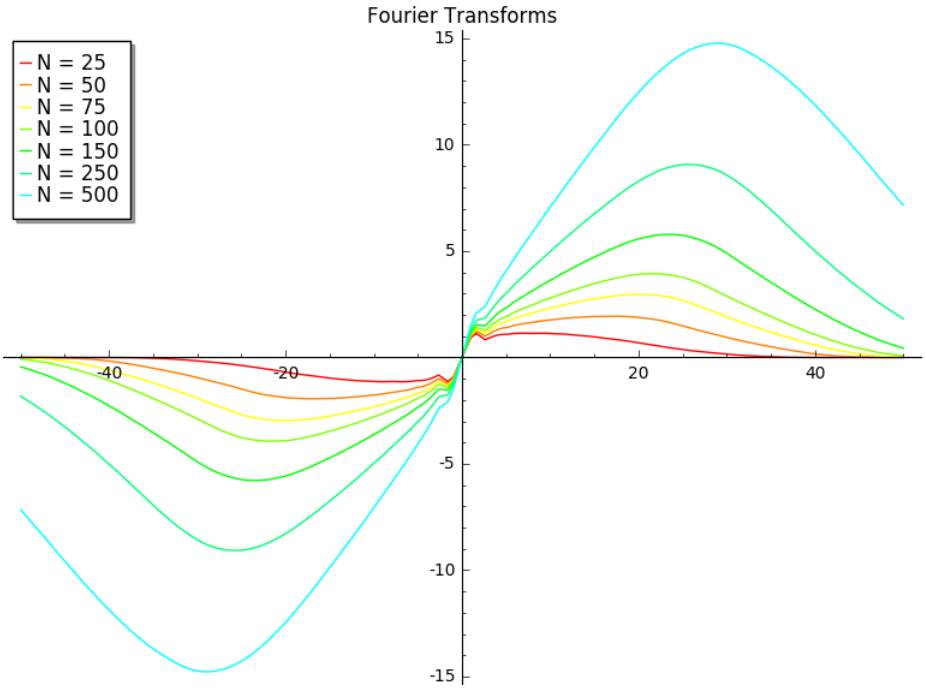

Figure 4.11. *Fourier transform of* $\sin(\alpha(m+n))$ *for* $(m,n) \in U_N$ *for various* N.

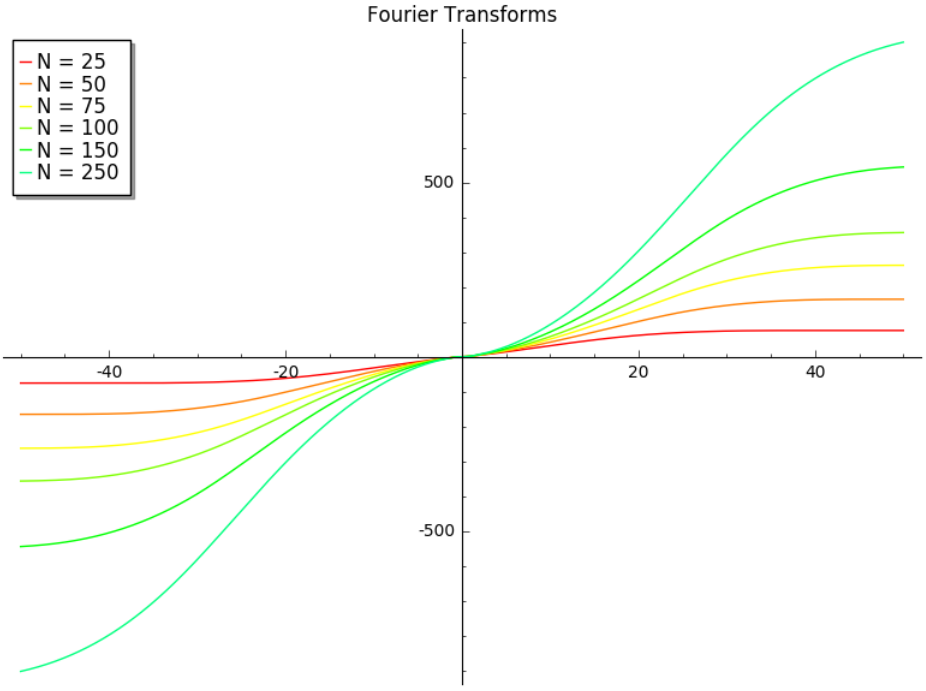

Figure 4.12. *Imaginary part of the Laplace transform of* $\cos(\alpha(m+n))$ *over* α *for* $(m,n) \in U_N$ *for various* N.

Except for the "sawtooth" points near the center of the graph over ω, it looks like we're getting exponentially-shaped distributions for the Fourier transforms. How do we compare this behavior to the theoretical asymptotic formula over the points above that we do know?

5. Questions

- How do we tell if we get a special non-uniform measure for a particular α in our case?
- Is it possible to connect the 1D Ulam set cases with the 2D ones?